Modeling of the Flow due to Double Rotations Causing Phenomenon of Negative Pressure

IVAN KAZACHKOV

Department of Energy Technology of the Royal Institute of Technology,
Brinellvägen 68, 10044, Stockholm,
SWEDEN

also with

Department of Information Technology, Physical, Mathematical and Economic Sciences,
Nizhyn Mykola Gogol State University,
Grafska Street 2, 16600, Nizhyn, Chernihivska Oblast,
UKRAINE

Abstract: - This paper is devoted to mathematical modeling and computational experiments of a flow with negative pressure. A previously unknown class of fluid flow under the action of counter-current centrifugal forces is in focus. Volumetric forces in a non-conducting fluid can arise from gravity, vibrations, or rotations. In this paper, we consider controlled variable volumetric forces in a system with two rotations around the vertical axis and the tangential axis of a horizontal disk rotating around the vertical axis. The study of the coordinate system during double rotation showed that the double rotation about two perpendicular axes, one of which moves along a tangential direction to the rotating horizontal disk, is equal to the rotation around the oscillating axis inclined at some angle to the vertical axis.

Key-Words: - Centrifugal Forces; Double Rotations; Curvilinear Gap; Stretching; Negative Pressure; Cavitation.

1 Introduction

A boundary value problem is formulated for a system of partial differential equations (Navier-Stokes), which describe the motion of fluid inside a turbine with the subsequent transition of its internal channel into the cavitation section, which has three parallel narrow slit cylindrical channels with curved walls and flow holes between channels (a patent of a Swedish company United Science and Capital Sweden AB, [1]). Then differential equation array is integrated across the narrow channel to simplify the equations. The resulting mathematical model allowed analyzing and creating the numerical method.

Mathematical and computer simulations revealed an intense oscillating fluid flow in a curved gap with periodic regions of negative and positive pressure due to constant and variable centrifugal forces. In the cross section of the channel, there is an area close to the outside of the turbine (with cavitator), where at high speeds of double rotation there is a stretching of the fluid by significant opposite centrifugal forces. The latter provides the conditions for an intense cavitation phenomenon, but due to the

negative pressure, other as yet unknown phenomena are also possible. Further development of the mathematical model is planned, as well as experimental study of these phenomena on the prepared device.

2 Statement by Flow under Double Rotations and Negative Pressure

2.1 Description of the System

The device, [1], is based on the principle of the cavitation process inside the working chamber (with the turbine at the entrance or without it in another version) due to the two high-speed independent rotations in two perpendicular directions.

The complex flow in the rotational channel placed on the rotating horizontal disk is considered according to the schematic in Figure 1, [1]. The first rotation is going around the z-axis as shown in Figure 1, with the rotation speed Ω. The other rotation has the rotation speed ω regarding the tangential axis to the main rotation circle, at the

distance R_0 from the central axis z (x=y=0) of the device.
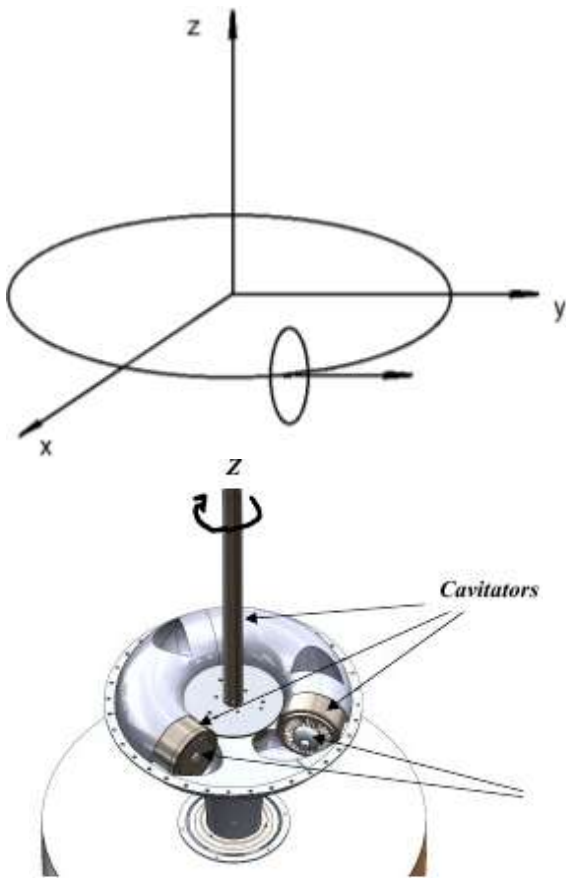

Fig. 1: Double rotating coordinate system for the device below: around vertical axis z and in channel around tangential axis to a circle of radius R_0

3 cavitators are rotating with the rotation speed ω installed around the axis z on the distance R_0 from the center, equally distributed by the circle of the radius R_0. Their radiuses are r_0.

The centrifugal forces in the turbines (cavitators) shown in Figure 2 are due to the main rotation (red color), the forces direct in all points of the flow to the left in the picture (edge of the main rotation circle). The centrifugal forces due to the turbine rotation (black) act along the radius of the turbine. Therefore, in situation 1 the centrifugal forces act in opposite directions causing a strong stretch of liquid (condition for the cavitation). To the left in the picture (situation 2), both forces act in the same direction creating the highest pressure (condition for a burst of cavitation bubbles). In all other places (e.g. 3 and 4) liquid moves from point 1 to point 2 counter-currently from the top and the bottom of the turbine.

2.2 Cylindrical Coordinates in the Channel

The rotating coordinate system has the vertical axis z or shifted from the central axis on some distance R_0 as shown in Figure 1. The rotation is going around the vertical axis z and also around the axis tangential to the circle of the radius R_0. Intensive rotation and mixing flow are fascinating phenomena and may be highly effective in several applications: engineering, technological, natural processes, [2], [3], [4], [5], [6].

Many theoretical aspects have been studied for the diverse rotational flows. Nevertheless, it is still a problem to learn more in deep for many theoretical, as well as practical applications. The described system with double rotations is considered at first in the world. In the local cylindrical coordinate system (r, φ, z) connected to the channel, the coordinate surfaces are cylinders $r = const$, semi-planes $\varphi = const$ and planes $z = const$. The focus of the paper is on the flow regimes in the gap of two rotating channels, therefore the coordinate z is now directed along the axis of the cylinder.
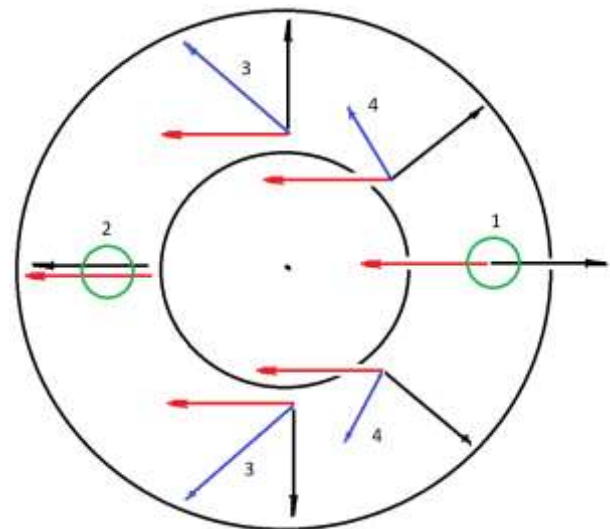

Fig. 2: Schematic of the centrifugal forces in the turbine

In Figure 1, we used z coordinate only for a general illustration of the system under consideration. But in the equations for the flow inside the turbine, the axis z is directed along the axis of the turbine, which is tangential to the rotating disk in the Figure 1.

2.3 Studies of Negative Pressure in Liquid

From the above analysis, the liquid may get into stretching conditions in some localities, where unknown dramatic regimes with negative pressure and cavitation are available. Normally cavitation is

supposed to be under depressurization below the saturation level, due to which liquid starts vaporizing. Negative pressure corresponds to a local stretching of liquid that can break the bonds of molecules causing the cavitation process to be much less known. A stretched liquid is under negative pressure. This is the unstable, metastable state of a liquid, possibly due to the Van der Waals forces of attraction between the molecules of the liquid: both, between themselves and between them and the walls of the vessel.

The gaseous state of a really existing substance, [7], is a gas that is not described exactly by the Clapeyron - Mendeleev equation, in contrast to its simplified model, hypothetical ideal gas. There is also another classification, according to which a highly superheated vapor is called a real gas, the state of which slightly differs from the state of an ideal gas. Superheated vapor, the state of which differs significantly from an ideal gas, and saturated vapor (two-phase equilibrium system liquid - vapor) does not obey the laws of an ideal gas, [7]. This phenomenon can be observed in the Torricelli experiment. Similarly, mercury in the medical thermometer, after the contact with the body has ceased, is in a stretched state. Moreover, it is in the maximum thermometer when the temperature begins dropping after the maximum, [8].

It is available to stretch the thoroughly cleaned and degassed water. In experiments, the short-term tensile stresses of 23-28 MPa were achieved, [9]. Technically pure liquids containing suspended solids and the smallest gas bubbles cannot withstand even minor tensile stresses. Nevertheless, this is a method of raising liquid working in trees, [10]. The superheated (metastable) liquid heated above its boiling point causes such specific dynamic phenomena as explosive boiling due to a stored heat, instability of liquid-vapor interface, and formation of a phase transition front in several regimes, [11].

Water is one of the substances that present density anomalies, [12], which may cause different unique phenomena, e.g. cavitation and abnormal behaviors. The negative pressure despite a long history of study is still a very little known phenomena, [13], [14], [15], [16], [17], [18], [19], [20], [21], [22], [23], [24], [25], [26], [27], e.g. paper, [11], shows that a high average stress difference on the interface of phase change is due to the negative stresses in the interface because the water belongs to a class of substances with density anomalies.

The negative pressure region of the phase diagram proves to be paramount in understanding the unusual behavior of this class of substances. Any condensed (solid or liquid) phase can exist in absolute negative pressure regimes, while the same is not true for gas phases. Theoretical arguments and experimental evidence demonstrated this. While in a gas phase pressure is proportional to density, this does not necessarily occur in condensed phases. It is convenient to extend the definition of pressure. In liquids and solids, pressure ought to be treated as 3x3- tensor **P**, rather than scalar, [14]. The authors [12] have shown how the negative pressure region of the phase diagram proves to be paramount in understanding the unusual behavior of this class of substances and in liquids and solids.

Several experiments made during the Royal Society Meeting, [15], did not provide any explanation for the experiment because adhesion and cohesion were not known for them yet. To generate a very high negative pressure in a liquid one ought to use extremely small amounts of sample, [16], [17], [18], [19], [20], [21], [22], [23], [24], [25]. The boiling of superheated and stretched liquids has been studied in a series of papers, [28], [29], [30], [31], [32]. The suppression effect for cavitation centers of a heterogeneous nature with low-boiling impurities was discovered experimentally. The effect of a pulsed electric field on the limiting overheating of liquid at negative pressures was revealed. It was shown that for short-term exposure to an electric field that does not lead to the formation of a noticeable amount of electrolysis products, the tension field of 10^7 V/cm is not enough to change the temperature of the limited liquid overheating.

2.4 Negative Pressure due Stretching Liquid
The physical situation described above by Figure 1 and Figure 2 revealed negative pressure oscillations due to a strong variation of the volumetric forces in a fluid flow by amplitude and direction. In the numerical simulation below, for the flow under double rotations, the amazing features (oscillations of flow parameters and pressure) from the high positive to the high negative values we revealed.

3 Mathematical Modelling of the Flow

3.1 Equations of Flow in Double Rotations
The differential equation array for the fluid flow in a cylindrical coordinate system is as follows, [33]:

$$\frac{\partial \rho}{\partial t} + \frac{\partial (\rho u)}{\partial r} + \frac{\rho u}{r} + \frac{\partial (\rho v)}{r \partial \varphi} + \frac{\partial (\rho w)}{\partial z} = 0,$$

$$\rho\left[\begin{array}{l}\frac{\partial u}{\partial t}+u\frac{\partial u}{\partial r}+\frac{v\partial u}{r\partial\varphi}+w\frac{\partial u}{\partial z}-\frac{v^2}{r}+r_0\omega^2+\\+(r_0\cos\varphi-R_0)\Omega^2\cos\varphi+2(v\omega-w\Omega\cos\varphi)\end{array}\right]=$$

$$=-\frac{\partial p}{\partial r}+\frac{\partial}{r^2\partial\varphi}(\mu\frac{\partial u}{\partial\varphi})++\frac{\partial}{\partial r}(\mu\frac{\partial u}{\partial r})+$$

$$+\frac{\partial}{\partial z}(\mu\frac{\partial u}{\partial z})+\frac{\partial(\mu u)}{r\partial r}-\frac{\mu}{r^2}\left(2\frac{\partial v}{\partial\varphi}+u\right),$$

$$\rho\left[\begin{array}{l}\frac{\partial v}{\partial t}+u\frac{\partial v}{\partial r}+\frac{v\partial v}{r\partial\varphi}+w\frac{\partial v}{\partial z}+\frac{uv}{r}+\\+(R_0-r_0\cos\varphi)\Omega^2\sin\varphi+2(w\Omega\sin\varphi-u\omega)\end{array}\right]=$$

$$=-\frac{1}{r}\frac{\partial p}{\partial\varphi}+\frac{\partial}{\partial r}(\mu\frac{\partial v}{\partial r})+\frac{\partial}{r^2\partial\varphi}(\mu\frac{\partial v}{\partial\varphi})+$$

$$+\frac{\partial}{\partial z}(\mu\frac{\partial v}{\partial z})+\frac{\partial(\mu v)}{r\partial r}+\frac{\mu}{r^2}(2\frac{\partial u}{\partial\varphi}-v),$$ (1)

$$\rho\left[\frac{\partial w}{\partial t}+u\frac{\partial w}{\partial r}+\frac{v\partial w}{r\partial\varphi}+w\frac{\partial w}{\partial z}+2\Omega(v\sin\varphi-u\cos\varphi)\right]=$$

$$=-\frac{\partial p}{\partial z}+\frac{\partial}{\partial r}(\mu\frac{\partial w}{\partial r})++\frac{\partial}{r^2\partial\varphi}(\mu\frac{\partial w}{\partial\varphi})+\frac{\partial}{\partial z}(\mu\frac{\partial w}{\partial z})+\frac{\partial(\mu w)}{r\partial r},$$

$$\rho c_v\left(\frac{\partial T}{\partial t}+u\frac{\partial T}{\partial r}+\frac{v\partial T}{r\partial\varphi}+\frac{w\partial T}{\partial z}\right)+p\left(\frac{\partial u}{\partial r}+\frac{u}{r}+\frac{\partial v}{r\partial\varphi}+\frac{\partial w}{\partial z}\right)=$$

$$=\frac{\partial}{\partial r}(\kappa\frac{\partial T}{\partial r})+\frac{\partial}{r^2\partial\varphi}(\kappa\frac{\partial T}{\partial\varphi})+\frac{\partial}{\partial z}(\kappa\frac{\partial T}{\partial z})+\frac{\partial(\kappa T)}{r\partial r}+Qc+$$

$$+\frac{\mu}{2}\left[\left(\frac{\partial u}{r\partial\varphi}-\frac{\partial v}{\partial r}-\frac{v}{r}\right)^2+\left(\frac{\partial v}{\partial z}+\frac{\partial w}{r\partial\varphi}\right)^2+\left(\frac{\partial w}{\partial r}+\frac{\partial u}{\partial z}\right)^2\right]+$$

.

where z is directed along the axis of the turbine. Here are: $\rho,\vec{v}=\{u,v,w\},p,T$ - density, velocity vector, pressure, and temperature, respectively, and, μ,κ - dynamic viscosity and heat conductivity coefficients, c_v- heat capacity, Q_c - internal heat generation due to cavitation.

3.2 Simplifications of the Model
We consider flow in a thin gap surrounding the wavy channel of the turbine rotating around its axis with a frequency ω so that centrifugal force is acting by the radius of the turbine; r_0 is the radius of the turbine. We neglect the width of the thin layer around the turbine in a narrow channel with wavy walls. The forces are projected on the coordinates r and φ, with account of the distance from the center of rotation.

4 Correlations for Curvilinear Channel
In the gap channel, we can simplify the equation array (1) due to small changes of the flow

parameters across the thin layer, transforming the problem from 3D to 2D geometry. The integration is performed by radial coordinate r across the channel's layer from one surface $\varepsilon_1=r_0+a\sin(k_r z)$ to another surface $\varepsilon_2=\varepsilon_1+b$. Here r_0 is the radius of the turbine without a curvilinear channel, a is the amplitude of the surface wave, b is the distance between the walls of the channel, $2\pi rdr$ is the integrating element in the cylindrical coordinate system.

4.1 Dimensionless Integral Correlations
For numerical modeling and simulation, it is better to use the equations in dimensionless form accepting the following scales for the velocity, length and pressure, correspondingly:

$$\omega r_0,\ r_0,\ 0.5\rho(\omega r_0)^2,$$

From (1), the dimensionless equations are got, [33]:

$$3\frac{\partial\bar{v}_0}{\partial\varphi}+2(\bar{b}+2)\frac{\partial\bar{w}_0}{\partial\bar{z}}=0,$$

$$\frac{\partial(\bar{v}_0\bar{u}_0)}{\partial\varphi}+\frac{4}{5}(2+\bar{b})\frac{\partial(\bar{v}_0\bar{u}_0)}{\partial\bar{z}}-\frac{4}{\bar{b}}\bar{v}_0^2=$$

$$=\frac{4}{\bar{b}}\left[2(\bar{b}+2)\gamma\bar{w}_0\cos\varphi-\bar{v}_0(\bar{b}+3)\right]+$$

$$+\frac{6}{\bar{b}}\left[2(1+\bar{a}\sin\alpha z)+\bar{b}\right]\left[(\beta-\cos\varphi)\gamma^2\cos\varphi-1\right],$$

$$\frac{\partial\bar{v}_0^2}{\partial\varphi}+2\left(1+\frac{2}{5}\bar{b}\right)\bar{w}_0\frac{\partial\bar{v}_0}{\partial\bar{z}}+3\frac{\partial\bar{p}}{\partial\varphi}=$$

$$=3\left[2(1+\bar{a}\sin\alpha\bar{z})+\bar{b}\right](\cos\varphi-\beta)\gamma^2\sin\varphi+$$

$$+\left[\bar{u}_0\bar{b}\left(\frac{\bar{b}}{2}+4\right)-2\gamma\bar{w}_0(\bar{b}+2)\sin\varphi\right]+$$ (2)

$$+\frac{1}{\text{Re}}\left[(\bar{b}+3)\frac{\partial^2\bar{v}_0}{\partial\bar{z}^2}-6\bar{a}\alpha^2\bar{v}_0\sin(\alpha\bar{z})\right]$$

$$\frac{\partial(\bar{v}_0\bar{w}_0)}{\partial\varphi}+\frac{4}{5}(2+\bar{b})\frac{\partial\bar{w}_0^2}{\partial\bar{z}}-\frac{\bar{b}}{5}\bar{u}_0\bar{w}_0+$$

$$+\frac{1}{2}\left[3(1+\bar{a}\sin\alpha\bar{z})+1.5\bar{b}\right]\frac{\partial\bar{p}}{\partial\bar{z}}=$$

$$=\gamma\left[\bar{u}_0\bar{b}\left(\frac{\bar{b}}{2}+4\right)\cos\varphi-\bar{v}_0(\bar{b}+3)\sin\varphi\right]+$$

$$+\frac{1}{\text{Re}}\left[6\left(2+\frac{1}{\bar{b}}\right)\frac{\partial^2\bar{w}_0}{\partial\varphi^2}+(\bar{b}+2)\frac{\partial^2\bar{w}_0}{\partial\bar{z}^2}\right]$$

.

Here are: $\bar{p}=p/(0.5\rho\omega^2r_0^2)$, $\text{Re}=\omega r_0^2/\nu$, $\bar{z}=z/r_0$, $\bar{b}=b/r_0$, $\bar{v}_0=v_0/(\omega r_0)$, $\bar{u}_0=u_0/(\omega r_0)$, $\bar{a}=a/r_0$, $\bar{w}_0=w_0/(\omega r_0)$, $\alpha=k_r r_0$, $\beta=R_0/r_0$, $\gamma=\Omega/\omega$.

4.2 The Parameters and Initial Conditions

The Reynolds number for our conditions ($r_0 = 6 sm$, $\omega = 18000 rpm$, $\nu = 10^{-6} m^2/s$) is $Re = 1.08 \cdot 10^6$, which means the highly developed turbulent flow, so that the turbulent viscosity must be accounted. If the "new Prandtl formula" is used, the above expression can be kept, with the turbulent viscosity coefficient.

The following initial data are stated:
Ω=6000 rpm, γ =1/3, a=1.5 mm, b=3 mm, $\bar{b}$ =0.05, β=3, α=60, k_r=10^3, $0.5\rho\omega^2 r_0^2$=162 kN/m²=162 kPa= 1.62 Bar. The water is supplied to the turbine by flow rate 1.7 l/s or 1.7 kg/s, so that by 6000 rpm at the R_0= 18 cm it creates the force 30.6 N, which is for the gap of the turbine by radius 6 cm and width 3 mm approximately P_0=(30.6/1.13)10^3 kN/m²=27.1 kPa. If the cross-section for the water supply is open only to the 10% of the total turbine cross-section, then P_0=271 kPa, or 2.71 Bar.

5 Solution of the Equation Array

5.1 Statement of the Boundary Problem

The equation array (2) was solved numerically by the following boundary conditions:

$$\bar{z} = 0, \quad \bar{u}_0 = 0, \quad \bar{w}_0 = -0.042, \quad \bar{v}_0 = 1, \quad \bar{p} = 1, \qquad (3)$$

satisfying the above considered physical situation.

Now all terms in (2) are estimated and the small ones are omitted compared to the bigger ones, to simplify the equations. Zero indexes are removed together with the tildes over the dimensionless functions, just for simplicity. Then it yields:

$$\frac{\partial vu}{\partial \varphi} + \frac{4}{5}(2+\varepsilon)\frac{\partial vu}{\partial z} - \frac{4}{\varepsilon}v^2 = \frac{4}{3}\left[2(\varepsilon+2)\gamma w \cos\varphi - v(\varepsilon+3)\right] +$$
$$+ \frac{6}{\varepsilon}\left[2(1+0.5\varepsilon\sin\alpha z)+\varepsilon\right]\left[(\beta-\cos\varphi)\gamma^2\cos\varphi - 1\right],$$

$$\frac{\partial v}{\partial \varphi} = -\frac{2}{3}(\varepsilon+2)\frac{\partial w}{\partial z}, \qquad (4)$$

$$\frac{\partial v^2}{\partial \varphi} + 2\left(1+\frac{2}{5}\varepsilon\right)w\frac{\partial v}{\partial z} + 3\frac{\partial p}{\partial \varphi} = 3\left[2(1+0.5\varepsilon\sin\alpha z)+\varepsilon\right](\cos\varphi-\beta)\gamma^2\sin\varphi +$$
$$+ \left[u\varepsilon\left(\frac{\varepsilon}{2}+4\right)-2\gamma w(\varepsilon+2)\sin\varphi\right] + \frac{1}{Re}\left[(\varepsilon+3)\frac{\partial^2 v}{\partial z^2} - 3\varepsilon\alpha^2 v\sin(\alpha z)\right],$$

$$\frac{\partial vw}{\partial \varphi} + \frac{4}{5}(2+\varepsilon)\frac{\partial w^2}{\partial z} - \frac{\varepsilon}{5}uw + \frac{1}{2}\left[3(1+0.5\varepsilon\sin\alpha z)+1.5\varepsilon\right]\frac{\partial p}{\partial z} =$$
$$= \gamma\left[u\varepsilon\left(\frac{\varepsilon}{2}+4\right)\cos\varphi - v(\varepsilon+3)\sin\varphi\right] +$$
$$+ \frac{1}{Re}\left[6\left(2+\frac{1}{\varepsilon}\right)\frac{\partial^2 w}{\partial \varphi^2} + (\varepsilon+2)\frac{\partial^2 w}{\partial z^2}\right],$$

where $\varepsilon = \bar{b}$, $\bar{a} = 0.5\varepsilon$.

5.2 The Non-Viscous Approximation

Because $Re = 1.08 \cdot 10^6$ by the estimation made, the non-viscous case (due to big inertia forces compared to the viscous ones) can be analyzed. For the stated parameters, neglecting $\varepsilon \approx 0.05$ in (4) compared to the 1 and similar, simplifies the (4) as follows:

$$\frac{\partial v}{\partial \varphi} = -\frac{4}{3}\frac{\partial w}{\partial z}, \quad \frac{\partial vu}{\partial \varphi} + \frac{8}{5}\frac{\partial vu}{\partial z} - 80v^2 = \frac{4}{3}\left[\frac{4}{3}w\cos\varphi - 3v\right] +$$
$$+ 240\left[(3-\cos\varphi)\frac{1}{9}\cos\varphi - 1\right], \qquad (5)$$

$$\frac{\partial v^2}{\partial \varphi} + 2w\frac{\partial v}{\partial z} + 3\frac{\partial p}{\partial \varphi} = \frac{2}{3}(\cos\varphi - 3)\sin\varphi + 4\left(\frac{u}{20} - \frac{1}{3}w\sin\varphi\right),$$

$$\frac{\partial vw}{\partial \varphi} + \frac{8}{5}\frac{\partial w^2}{\partial z} - 0.01uw + \frac{3}{2}\frac{\partial p}{\partial z} = \frac{1}{3}\left(\frac{u}{5}\cos\varphi - 3v\sin\varphi\right).$$

But $\frac{\partial vu}{\partial \varphi} + \frac{8}{5}\frac{\partial vu}{\partial z} \square\; 80v^2$ because $u \ll v$, therefore, from the first equation (5), follows:

$$v^2 = 3 - \cos\varphi + 1/3\cos^2\varphi + v/20 - w/45\cos\varphi.$$

Here $v/20$ and $w/45\cos\varphi$ may be of the same order if w grows dramatically inside the turbine compared to v. But there are no reasons for this. At the entrance to a turbine, they are respectively 0.05 and -0.00093. Therefore, finally, it yields:

$$v^2 - v/20 - \left(3 + 1/3\cos^2\varphi - \cos\varphi\right) = 0.$$

The solution of this algebraic equation yields

$$v = \frac{1}{40} \pm \sqrt{\frac{1}{1600} + 3 + \frac{1}{3}\cos^2\varphi - \cos\varphi} \approx \frac{1}{40}$$
$$\pm\sqrt{3 + \frac{1}{3}\cos^2\varphi - \cos\varphi} = \frac{1}{40} \pm \sqrt{2 + 2\sin^2\frac{\varphi}{2} + \frac{1}{3}\cos^2\varphi} \qquad (6)$$

5.3 Phenomenon of Two Counter-Current Rotational Flows under Double Rotations

As the correlation (6) shows, there are two counter-current rotational flows with approximately the same velocities, which correspond to the analysis of physical processes, namely the action of the resulting centrifugal force from the line φ=0 to the φ=π from the top and from the bottom, both sides (as shown in Figure 2):

$$\varphi = 2\pi n, \quad v = \frac{1}{40} \pm 1.53; \quad \varphi = \frac{\pi}{2} + \pi n, \quad v = \frac{1}{40} \pm 1.73;$$

$$\varphi = \pi(2n+1), \quad v = \frac{1}{40} \pm 2.08; \qquad (7)$$

where $n = 0, \pm 1, \pm 2, \pm 3, \dots$ The plus-minus in (6), (7), and later on correspondingly to the counter-current flows going in the opposite directions from the plane $\varphi=0$, symmetrically pushing the fluid from $\varphi=0$ to $\varphi=\pi$.

This is a very unusual complex flow due to the double rotations, which cause centrifugal forces in the flow inside the turbine, when all the fluid is pushed in the cross-section from $\varphi=0$ to $\varphi=\pi$ and along the symmetry axis to the exit of the turbine. All the time, due to the rotation of the turbine, the new portion of water is coming from $\varphi=0$ to $\varphi=\pi$.

Then derivative $\partial v / \partial \varphi$ from (6) and put into (5):

$$\frac{\partial w}{\partial z} = \mp \frac{3\sin\varphi - \sin 2\varphi}{8\sqrt{2 + 2\sin^2\frac{\varphi}{2} + \frac{1}{3}\cos^2\varphi}}, \qquad (8)$$

$$w = \mp \frac{3\sin\varphi - \sin 2\varphi}{8\sqrt{2 + 2\sin^2\frac{\varphi}{2} + \frac{1}{3}\cos^2\varphi}} z - 0.042 + A_1(\varphi),$$

$\varphi = 2\pi n, \quad w = -0.042; \qquad \varphi = \frac{\pi}{2} + \pi n, \quad w = -0.042 \mp 0.22z;$

$\varphi = \pi(2n+1), \quad w = -0.042;$

where $A_1(\varphi)$ - an arbitrary function of φ computed from (3), $n = 0, \pm 1, \pm 2, \pm 3, \dots$ $A_1(\varphi) = 0$ if no initial distribution by φ is stated for w. As seen from (8), the velocity of the component flow along the axis of the turbine is always in the same direction and the same amplitude as from the inlet $w = -0.042$. But at the upper and bottom points of the turbine ($\varphi = \pm\pi/2$) it has two components: $w = -0.042 - 0.216z$, $w = -0.042 + 0.216z$, respectively, which give at $z=-1$, correspondingly, $w = 0.174$ and $w = -0.258$.

5.4 Calculation of the Flow Pressure

From the third equation of the system (5), where it is possible to neglect the term $2w\partial v / \partial z$ comparing to the $\partial v^2 / \partial\varphi$ because $w \ll 1$ and $\partial v / \partial z \approx 0$, yields

$$\frac{\partial p}{\partial\varphi} = -\frac{1}{3}\frac{\partial v^2}{\partial\varphi} + \frac{2}{9}(\cos\varphi - 3)\sin\varphi + \frac{4}{3}\left(\frac{u}{20} - \frac{w}{3}\sin\varphi\right),$$

As far as $u \ll w$, we can neglect the term $u/20$ in the above equation as the small one comparing to the $w/3\sin\varphi$, and then omit $4w/9\sin\varphi$ comparing to $2/3\sin\varphi$ (also because we have no part of the w in (8), which is responsible for the dependence of w on φ). Therefore, it results in

$$\frac{\partial p}{\partial\varphi} = -\frac{1}{3}\frac{\partial v^2}{\partial\varphi} + \frac{2}{9}(\cos\varphi - 3)\sin\varphi,$$

where from follows after partial integration by angle coordinate φ, with account of (6), (8):

$$p = -\frac{1}{3}\left(\frac{1}{40} \pm \sqrt{2 + 2\sin^2\frac{\varphi}{2} + \frac{1}{3}\cos^2\varphi}\right)^2 +$$
$$-\frac{1}{9}\cos^2\varphi + 0.67\cos\varphi + C_1(z) \qquad (9)$$

And the total pressure is got as total integral from the total differential:

$$dp = \frac{\partial p}{\partial\varphi}d\varphi + \frac{\partial p}{\partial z}dz. \qquad (10)$$

Therefore, let us compute also partial integral by coordinate z using the last equation of the system (5).

The second partial integral (now it is by coordinate z) is got according to (10):

$$p = \frac{2uz}{45}\cos\varphi - \frac{2}{3}\sin\varphi\left(\frac{1}{40} \pm \sqrt{2 + 2\sin^2\frac{\varphi}{2} + \frac{1}{3}\cos^2\varphi}\right)z +$$
$$-2.8 \cdot 10^{-4}uz + \left(\frac{\cos\varphi}{8} - \frac{\cos 2\varphi}{12}\right)z^2 +$$
$$\pm \frac{4.7 \cdot 10^{-3}(3\sin\varphi - \sin 2\varphi)z}{\sqrt{2 + 2\sin^2\frac{\varphi}{2} + \frac{1}{3}\cos^2\varphi}} \pm 1.04 \cdot 10^{-3}\frac{\partial\Phi}{\partial\varphi} \cdot z^2 + C_2(r) +$$
$$\mp 4.2 \cdot 10^{-4}\frac{(3\sin\varphi - \sin 2\varphi)z^2}{\sqrt{2 + 2\sin^2\frac{\varphi}{2} + \frac{1}{3}\cos^2\varphi}} + \qquad (11)$$
$$-\frac{16}{15}\left[0.042 \pm \frac{(3\sin\varphi - \sin 2\varphi)z}{\sqrt{2 + 2\sin^2\frac{\varphi}{2} + \frac{1}{3}\cos^2\varphi}}\right]^2.$$

$C_2(r)$ is got from boundary conditions. Finally,

$$p = -\frac{1}{3}\left(\frac{1}{40} \pm \sqrt{2 + 2\sin^2\frac{\varphi}{2} + \frac{1}{3}\cos^2\varphi}\right)^2 +$$
$$-\frac{2}{3}\sin\varphi\left(\frac{1}{40} \pm \sqrt{2 + 2\sin^2\frac{\varphi}{2} + \frac{1}{3}\cos^2\varphi}\right)z +$$
$$+0.67\cos\varphi + \frac{2uz}{45}\cos\varphi - \frac{1}{9}\cos^2\varphi - 2.8 \cdot 10^{-4}uz + \left(\frac{\cos\varphi}{8} - \frac{\cos 2\varphi}{12}\right)z^2 + \qquad (12)$$
$$\mp 4.2 \cdot 10^{-4}\frac{(3\sin\varphi - \sin 2\varphi)z^2}{\sqrt{2 + 2\sin^2\frac{\varphi}{2} + \frac{1}{3}\cos^2\varphi}} +$$
$$-\frac{16}{15}\left[0.042 \pm \frac{(3\sin\varphi - \sin 2\varphi)z}{\sqrt{2 + 2\sin^2\frac{\varphi}{2} + \frac{1}{3}\cos^2\varphi}}\right]^2 \pm 1.04 \cdot 10^{-3}\frac{\partial\Phi}{\partial\varphi} \cdot z^2 +$$

$$\pm \frac{4.7 \cdot 10^{-3}\left(3\sin\varphi - \sin 2\varphi\right)z}{\sqrt{2 + 2\sin^2 \frac{\varphi}{2} + \frac{1}{3}\cos^2\varphi}} +$$

$$\pm 0.055 z \int \frac{\left(3\sin\varphi - \sin 2\varphi\right)\sin\varphi}{\sqrt{2 + 2\sin^2 \frac{\varphi}{2} + \frac{1}{3}\cos^2\varphi}} d\varphi + C_1(z) + C_2(r)$$

The (9), and (11) were inserted into (10) yielding the total pressure distribution (12) by the coordinates z and φ. By the coordinate z, $C_1(z)$ is easily computed according to the boundary condition (3), while the pressure distribution at the inlet to the turbine $C_2(r)$ is not so simple question, therefore, we put $C_2(r) = 0$. Then pressure distribution in the turbine flow is:

$$p = 1 - \frac{1}{3}\left(\frac{1}{40} \pm \sqrt{2 + 2\sin^2 \frac{\varphi}{2} + \frac{1}{3}\cos^2\varphi}\right)^2 +$$

$$- \frac{2}{3}\sin\varphi\left(\frac{1}{40} \pm \sqrt{2 + 2\sin^2 \frac{\varphi}{2} + \frac{1}{3}\cos^2\varphi}\right)z +$$

$$+ 0.67\cos\varphi + \frac{2uz}{45}\cos\varphi - \frac{1}{9}\cos^2\varphi - 2.8 \cdot 10^{-4} uz + \left(\frac{\cos\varphi}{8} - \frac{\cos 2\varphi}{12}\right)z^2 + \quad (13)$$

$$\mp 4.2 \cdot 10^{-4} \frac{\left(3\sin\varphi - \sin 2\varphi\right)z^2}{\sqrt{2 + 2\sin^2 \frac{\varphi}{2} + \frac{1}{3}\cos^2\varphi}} +$$

$$- \frac{16}{15}\left[0.042 \pm \frac{\left(3\sin\varphi - \sin 2\varphi\right)z}{\sqrt{2 + 2\sin^2 \frac{\varphi}{2} + \frac{1}{3}\cos^2\varphi}}\right]^2 \pm 1.04 \cdot 10^{-3} \frac{\partial \Phi}{\partial \varphi} \cdot z^2 +$$

$$\pm \frac{4.7 \cdot 10^{-3}\left(3\sin\varphi - \sin 2\varphi\right)z}{\sqrt{2 + 2\sin^2 \frac{\varphi}{2} + \frac{1}{3}\cos^2\varphi}} \pm 0.055 z \int \frac{\left(3\sin\varphi - \sin 2\varphi\right)\sin\varphi}{\sqrt{2 + 2\sin^2 \frac{\varphi}{2} + \frac{1}{3}\cos^2\varphi}} d\varphi$$

.

6 Computer Simulation

6.1 Analysis of the Terms in Solution and Simplification of the Model

In the equation (13), the following terms may be omitted as the small ones comparing to the other similar terms:

$$\mp 4.2 \cdot 10^{-4} \frac{\left(3\sin\varphi - \sin 2\varphi\right)z^2}{\sqrt{2 + 2\sin^2 \frac{\varphi}{2} + \frac{1}{3}\cos^2\varphi}}, \quad 2.8 \cdot 10^{-4} uz,$$

$$\pm 1.04 \cdot 10^{-3} \frac{\partial \Phi}{\partial \varphi} \cdot z^2, \quad \pm \frac{4.7 \cdot 10^{-3}\left(3\sin\varphi - \sin 2\varphi\right)z \cdot}{\sqrt{2 + 2\sin^2 \frac{\varphi}{2} + \frac{1}{3}\cos^2\varphi}}$$

Then the equation (13) is simplified as follows:

$$p = 1 - \frac{1}{3}\left(\frac{1}{40} \pm \sqrt{2 + 2\sin^2 \frac{\varphi}{2} + \frac{1}{3}\cos^2\varphi}\right)^2 +$$

$$+ 0.67\cos\varphi - \frac{1}{9}\cos^2\varphi + \left[\frac{2u}{45}\cos\varphi +\right.$$

$$- \frac{2}{3}\sin\varphi\left(\frac{1}{40} \pm \sqrt{2 + 2\sin^2 \frac{\varphi}{2} + \frac{1}{3}\cos^2\varphi}\right) + \quad (14)$$

$$\mp 0.022 \frac{3\sin\varphi - \sin 2\varphi}{\sqrt{2 + 2\sin^2 \frac{\varphi}{2} + \frac{1}{3}\cos^2\varphi}} +$$

$$\left. \pm 0.055 \int \frac{\left(3\sin\varphi - \sin 2\varphi\right)\sin\varphi}{\sqrt{2 + 2\sin^2 \frac{\varphi}{2} + \frac{1}{3}\cos^2\varphi}} d\varphi \right] z +$$

.

$$+ \left[\frac{\cos\varphi}{8} - \frac{\cos 2\varphi}{12} - 1.07 \frac{\left(3\sin\varphi - \sin 2\varphi\right)^2}{2 + 2\sin^2 \frac{\varphi}{2} + \frac{1}{3}\cos^2\varphi}\right] z^2$$

6.2 Preliminary Analysis of Flow Peculiarities

The obtained correlation (14) describes the pressure distribution in the two flows: up and down of the turbine from its right side to its left side. At the entrance there is about 25% loses comparing to the pressure in front of the turbine. The turbine is rotating but the liquid is flowing counter-currently from $\varphi = 0$ to $\varphi = \pi$ from the top and to $\varphi = -\pi$ from the bottom of the turbine due to the double centrifugal forces, which move the liquid both sides of the turbine to the region $\varphi = \pm\pi$, where from it is pressurized and pushed along the axis to the exit of turbine.

The upper sign in the "plus-minus" expressions of (13) correspond respectively to the upper and down flows in the turbine. Therefore, we assume that at the plane $\varphi = 0$, where the pressures are subtracting each other and velocities are counter-current, the liquid is stretched by plus and minus forces, so that cavitation may happen. But at the meeting point of the two counter-current flows at the plane $\varphi = \pm\pi$, the pressure is doubled due to a meeting of two opposite flows. Thus, according to the above, from the (13) yields the following pressure difference at $\varphi = 0$:

$$p_+ - p_- = -\left(1/30\right)\sqrt{7/3} \approx -0.05$$

Here, the pressure is 0.56 and the total pressure (with an account of dynamic pressure) is 2.9. The dynamic pressures are the same acting in counter-current directions resulting in zero. Thus, the opposite flows and negative pressure are good

condition for the cavitation. At the upper and downsides of the turbine $\varphi = \pm\pi/2$, the pressure is 0 and the total pressure is 3.0. At the external part of turbine, $\varphi = \pm\pi$, the pressure is -4.11 and the total pressure, with account of the two meeting counter-current flows with the dynamic pressures 4.32, is 4.53!

As seen from the above estimation, due to the counter-current flow by the coordinate φ, the flow pressure in the turbine is substantially decreased (depressurized flow) to the side of turbine $\varphi = 0$, while it is increased (pressurized) to the opposite side of the turbine ($\varphi = \pi$). Then up and down of the turbine ($\varphi = \pm\pi/2$), it is symmetrically prone to a slight pressurization.

The pressure difference between the sections $\varphi = \pm\pi/2$, $\varphi = 0$ is $\Delta p = -0.56$, and between the sections $\varphi = \pi$ and $\varphi = \pm\pi/2$ it is $\Delta p = -4.11$, so that flow is intensively accelerated in the last semi-sphere. We estimate dependence of the pressure on longitudinal coordinate z, which is negative due to a liquid flow opposite to the turbine movement by tangential to the main rotation circle. For the $z=-1$, from (14) follows:

$$p = 1 - \frac{1}{3}\left(\frac{1}{40} \pm \sqrt{2 + 2\sin^2\frac{\varphi}{2} + \frac{1}{3}\cos^2\varphi}\right)^2 +$$

$$+0.67\cos\varphi - \frac{1}{9}\cos^2\varphi - \frac{2u}{45}\cos\varphi +$$

$$+\frac{2}{3}\sin\varphi\left(\frac{1}{40} \pm \sqrt{2 + 2\sin^2\frac{\varphi}{2} + \frac{1}{3}\cos^2\varphi}\right) +$$

$$\pm 0.022\frac{3\sin\varphi - \sin 2\varphi}{\sqrt{2 + 2\sin^2\frac{\varphi}{2} + \frac{1}{3}\cos^2\varphi}} +$$

$$\mp 0.055\int\frac{(3\sin\varphi - \sin 2\varphi)\sin\varphi}{\sqrt{2 + 2\sin^2\frac{\varphi}{2} + \frac{1}{3}\cos^2\varphi}}d\varphi + \frac{\cos\varphi}{8} +$$

$$-\frac{\cos 2\varphi}{12} - 1.07\frac{(3\sin\varphi - \sin 2\varphi)^2}{2 + 2\sin^2\frac{\varphi}{2} + \frac{1}{3}\cos^2\varphi}.$$

(15)

Neglecting the small terms in (15) yields

$$p = \frac{1}{3} - \frac{1}{3}\left(2\sin^2\frac{\varphi}{2} + \frac{1}{3}\cos^2\varphi\right) + 0.79\cos\varphi - \frac{1}{9}\cos^2\varphi - \frac{\cos 2\varphi}{12} +$$

$$\pm\frac{2}{3}\sin\varphi\sqrt{2 + 2\sin^2\frac{\varphi}{2} + \frac{1}{3}\cos^2\varphi} - 1.07\frac{(3\sin\varphi - \sin 2\varphi)^2}{2 + 2\sin^2\frac{\varphi}{2} + \frac{1}{3}\cos^2\varphi}$$

and calculation gives:

$\varphi=0$: $p=0.82$; $\varphi = \pm\pi/2 : p=-1.97$; $\varphi = \pm\pi : p=-1.43$.

The pressure difference between the sections $\varphi = \pm\pi/2$ and $\varphi=0$ is $\Delta p = -2.79$, between the sections $\varphi = \pi$ and $\varphi = \pm\pi/2$ it is $\Delta p = 0.54$, so that the water flow is shifted to a middle section of the turbine $\varphi = \pi$ close to the axis at the exit.

6.3 Computer Simulation of the Flow

The approximate models (6), (8), and (13) were also implemented for the computer simulation in a wide range of parameters using the prepared FLEX PDE computer program. This is compared to the full model.

As numerical simulations showed, the above approximate mathematical model is unique in the point that it allowed revealing the counter-current flow in a rotational turbine while direct numerical simulation on the computer does not allow this because the numerical solution cannot treat simultaneous flow in two opposite directions (two different solutions at the same time!). A combination of the detailed analysis of the approximate analytical solution and direct computer simulation is important because it allows revealing all possible regimes of the device functioning.

In a curvilinear channel, the radial velocity can be estimated through the following correlation taking into account the form of the channel: $r = b + a\sin kz$. Thus, $u = \partial r/\partial t = ak\cos kz \cdot \partial z/\partial t = ak\cos kz \cdot w$, which yields for $a=1.5$ mm, $k=628$, $k10^{-2} = 2\pi$, one wave on 1 cm length of the channel, the following estimation: $u = w\cos kz$.

Now, accounting (5), and (6), with this estimation for the radial oscillating velocity, let us take approximate pressure from (14) neglecting the estimated small terms and considering separately the solutions for the upper and the down parts of the turbine, correspondingly:

$$\frac{\partial v^2}{\partial\varphi} + 2w\frac{\partial v}{\partial z} + 3\frac{\partial p}{\partial\varphi} = \frac{2}{3}(\cos\varphi - 3)\sin\varphi + 4\left(\frac{u}{20} - \frac{1}{3}w\sin\varphi\right),$$

$$p = \frac{1}{3} - \frac{2}{3}\sin^2\frac{\varphi}{2} - \frac{1}{60}\sqrt{2 + 2\sin^2\frac{\varphi}{2} + \frac{1}{3}\cos^2\varphi} +$$

$$+0.67\cos\varphi - \frac{2}{9}\cos^2\varphi + \left[\frac{2w}{45}\cos kz\cos\varphi +\right.$$

$$-\frac{2}{3}\sin\varphi\sqrt{2 + 2\sin^2\frac{\varphi}{2} + \frac{1}{3}\cos^2\varphi} +$$

$$\left.-0.022\frac{3\sin\varphi - \sin 2\varphi}{\sqrt{2 + 2\sin^2\frac{\varphi}{2} + \frac{1}{3}\cos^2\varphi}}\right]z +$$

(16)

$$+\left[\frac{\cos\varphi}{8}-\frac{\cos 2\varphi}{12}-1.07\frac{\left(3\sin\varphi-\sin 2\varphi\right)^2}{2+2\sin^2\frac{\varphi}{2}+\frac{1}{3}\cos^2\varphi}\right]z^2,$$

$$v=\frac{1}{40}+\sqrt{2+2\sin^2\frac{\varphi}{2}+\frac{1}{3}\cos^2\varphi};$$

$$\frac{\partial v^2}{\partial\varphi}+2w\frac{\partial v}{\partial z}+3\frac{\partial p}{\partial\varphi}=\frac{2}{3}(\cos\varphi-3)\sin\varphi+4\left(\frac{u}{20}-\frac{1}{3}w\sin\varphi\right),$$

$$p=\frac{1}{3}-\frac{2}{3}\sin^2\frac{\varphi}{2}+\frac{1}{60}\sqrt{2+2\sin^2\frac{\varphi}{2}+\frac{1}{3}\cos^2\varphi}+$$

$$+0.67\cos\varphi-\frac{2}{9}\cos^2\varphi+\left[\frac{2w}{45}\cos kz\cos\varphi+\right.$$

$$+\frac{2}{3}\sin\varphi\sqrt{2+2\sin^2\frac{\varphi}{2}+\frac{1}{3}\cos^2\varphi}+$$

(17)

$$\left.+0.022\frac{3\sin\varphi-\sin 2\varphi}{\sqrt{2+2\sin^2\frac{\varphi}{2}+\frac{1}{3}\cos^2\varphi}}\right]z+$$

$$+\left[\frac{\cos\varphi}{8}-\frac{\cos 2\varphi}{12}-1.07\frac{\left(3\sin\varphi-\sin 2\varphi\right)^2}{2+2\sin^2\frac{\varphi}{2}+\frac{1}{3}\cos^2\varphi}\right]z^2,$$

$$v=\frac{1}{40}-\sqrt{2+2\sin^2\frac{\varphi}{2}+\frac{1}{3}\cos^2\varphi}.$$

The equation arrays (16) and (17) for the upper and down parts of the turbine were solved numerically.

6.4 The Results of Computer Simulation

The results of calculations for regions $0\leq\varphi\leq\pi$, $-\pi\leq\varphi\leq 0$ and a few cross-sections of the channel in the range $-3\leq z\leq 0$ are given below. By the upper part of the channel according to (16) are presented in Figure 3, Figure 4 and Figure 5 (x is assigning the variable φ in the graphs).

Thus, flow in the channel at section z=-0.5 is along the axis of the channel only in a vicinity of φ=0. In the main volume, it oscillates decreasing the flow rate along the axis. What is more, with an account of the sharp pulses close to the opposite side of the channel (φ=π) it may be concluded that at this cross-section, at the distance z=-0.5, the flow rate is nearly zero (just shaking along the axis).
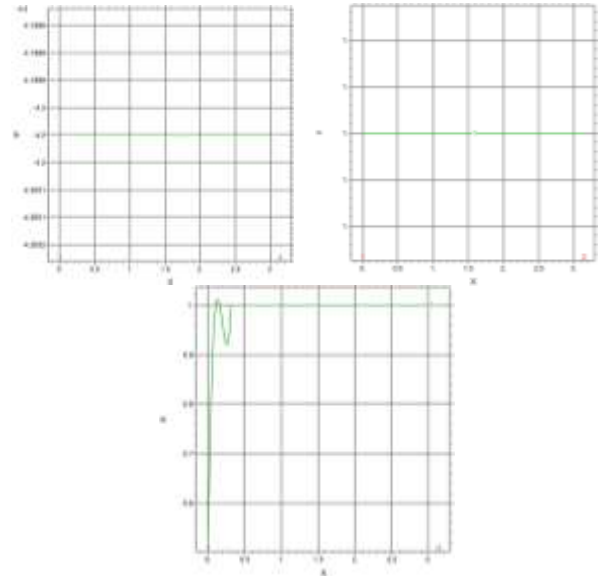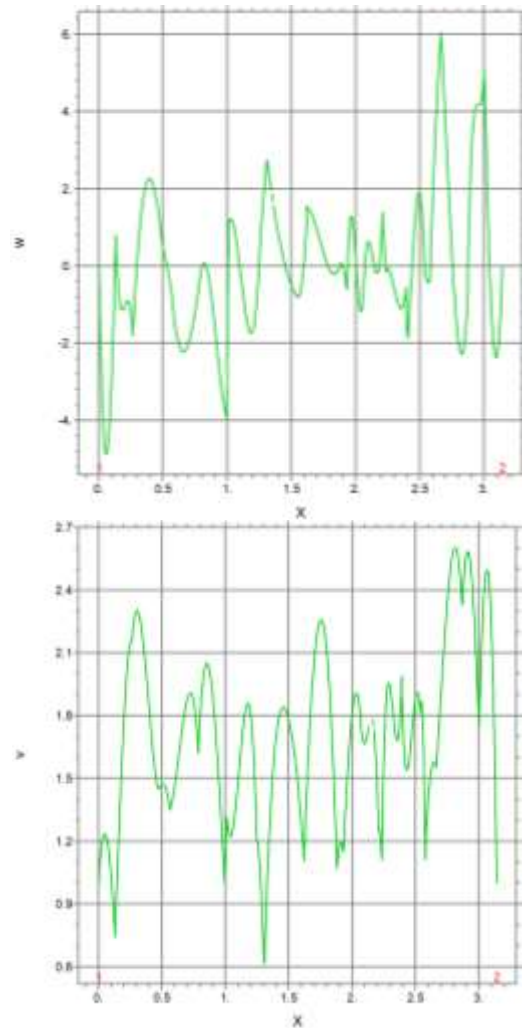

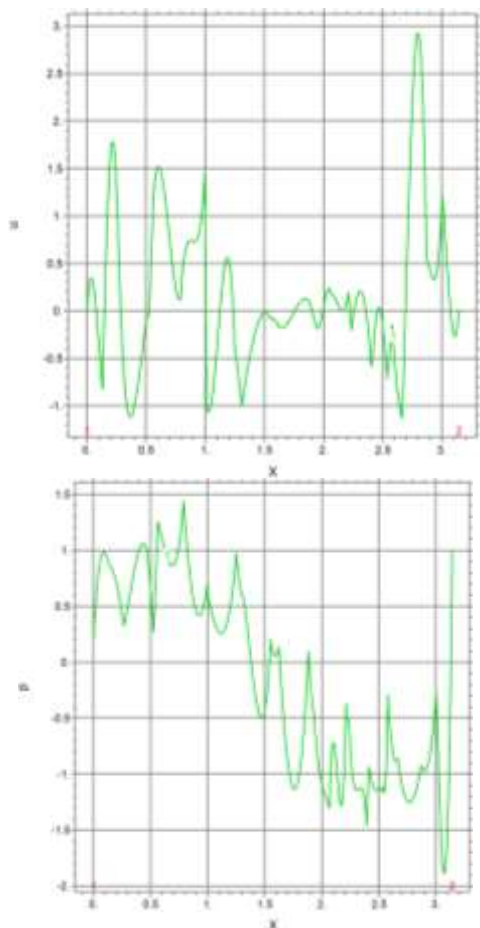Fig. 3: Initial data w,v,u,p at turbine's entrance (z=0)

Fig. 4: Flow parameters *w, v, u, p* at *z*=-0.5 depending on $0 \leq \varphi \leq \pi$ (in radians, from 0 to 3.14)

The rotational velocity *v* has every positive direction being substantially oscillating. Flow pressure oscillates a lot being negative in half of the cross-section.

Figure 5 shows a similar tendency by *z*=-1 but the axial velocity has a lower peak close to φ=0 (w=-3.6) but a big negative peak at φ =0.86π (w=-6).
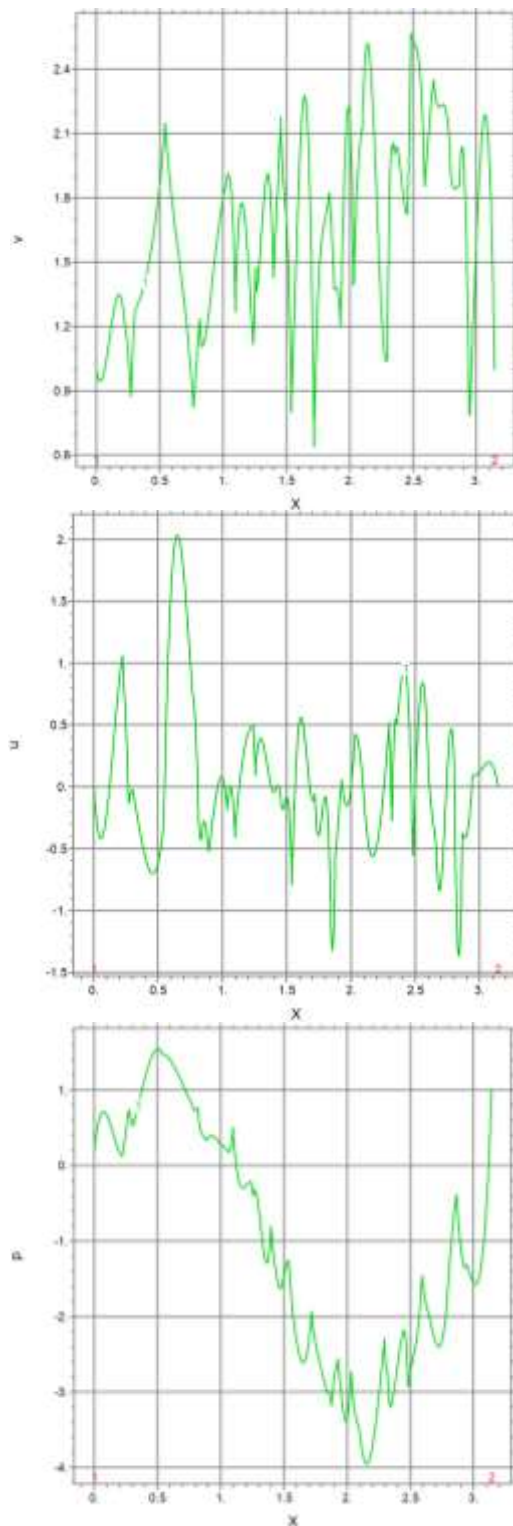

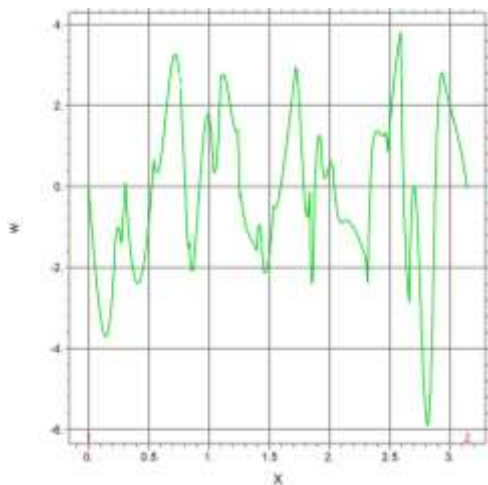Fig. 5: Flow parameters *w, v, u, p* at the cross-section *z*=-1 depending on angle $0 \leq \varphi \leq \pi$

Mostly it oscillates in range (-2, 3), and integrally very little flow rate along the axis, prevailing oscillation. The rotational velocity v has everywhere positive direction being even more oscillating than before, with increase of the amplitude from φ =0 to φ =π.

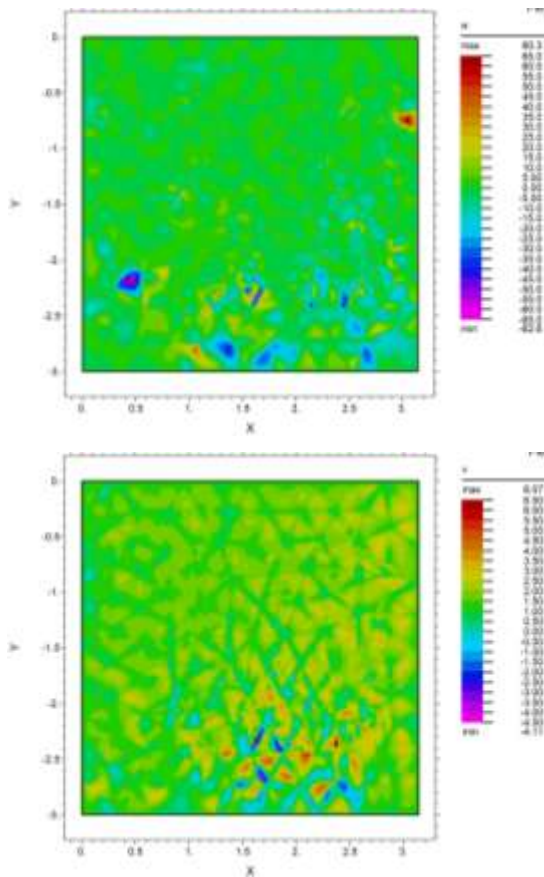Fig. 6: Axial and rotational flow velocities in channel by z,φ (y,x in figure)
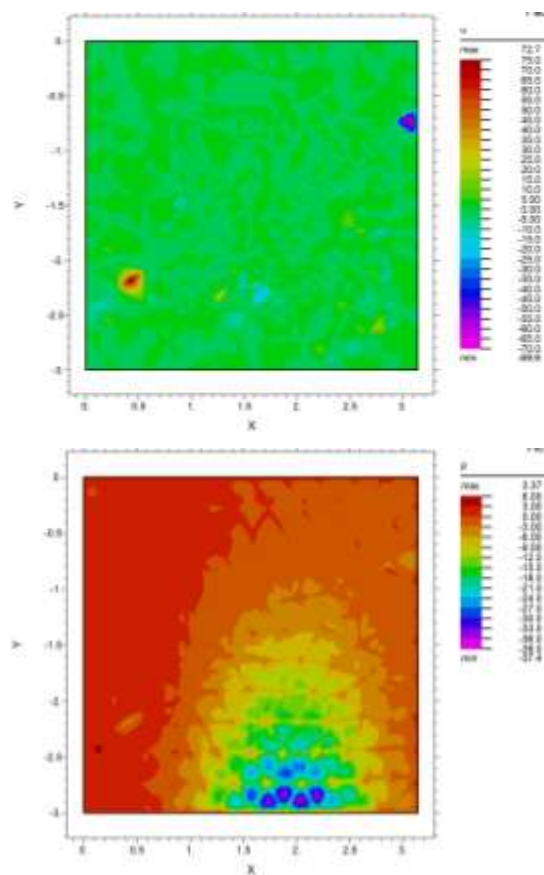

Fig. 7: Cross-sectional velocity-pressure by z,φ (y,x)

The flow pressure is higher than at $z=-0.5$ and the negative pressure region is bigger (more than half of the whole section and up to $p=-4$ around $\varphi=0.68\pi$). The general tendency of the longitudinal and rotational velocities is given by both coordinates in the region in Figure 6, where from is seen that the most impressive anomalies are at the end of the channel.

Similarly, the cross-sectional velocity and pressure in the region are presented in Figure 7, where it is obvious that the region of negative pressure is mostly approximately after a distance of one radius of the channel. It is quite big and the highest values are at the end of the channel from $\varphi=\pi/2$ to $\varphi=3\pi/4$. At the beginning of the channel, the negative pressure is absent. The highest positive pressure is in the range of approximately $\varphi=0$ to $\varphi=\pi/4$ in the whole channel.

The flow parameters at the exit from the channel are given for the presented simulation in Figure 8.
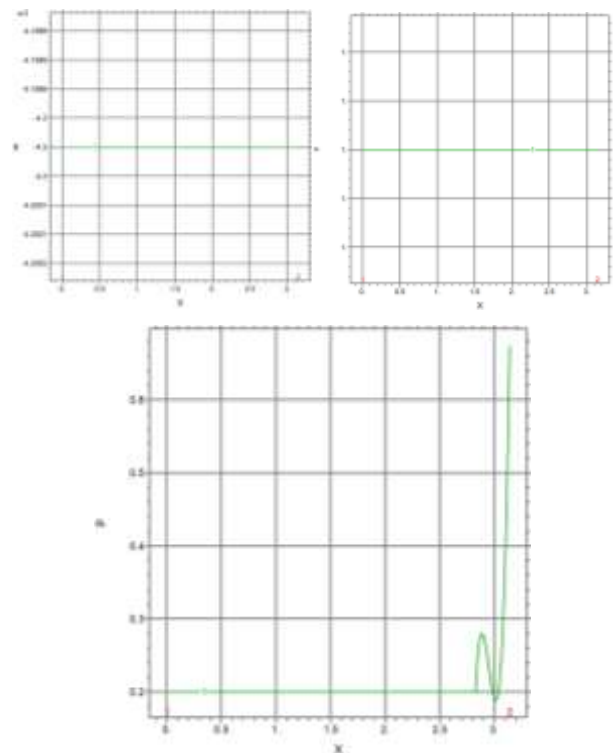

Fig. 8: Flow parameters w,v,u,p at exit ($z=-3$)

7 Conclusion

The developed mathematical model and the computer simulation have shown the peculiarities of the thermal hydraulic processes inside the device under double rotations. The governing parameters are all interconnected and are sensitive to variation. After obtaining the first experimental data it is

possible to solve the problem of optimization of the main parameters of the processes and device. This is the base for the calculation of the optimal parameters in further industrial construction.

The control parameters are the speed of rotation and flow rate. As it is seen from the data obtained, in the turbine, there is an available pressure increase of up to 5 times compared to the entering pressure to the turbine. Using the developed models and computer programs it is possible to perform detailed calculations and optimization of the processes based on the experimental data. Express analysis of the requested parameters is available even in a notebook.

The most remarkable is that the abrupt increase of the pressure locally due to the cavitation process does not influence the whole region but just locally as a concern to pressure. The velocity components are growing substantially and oscillating a lot. This means that such intensive spatial variation of the flow parameters creates the conditions for the production of the cavitation bubbles in the internal part of the turbine where a huge decrease of the pressure happens, while in the opposite part of the turbine, the dramatic increase of pressure leads to explosion of the bubbles causing the intensive fluid heating.

The mathematical model allows studying the main regularities of a new class of problems related to the flow in channels under the influence of double rotations, in which volumetric variable centrifugal forces arise. The centrifugal forces create significant oscillations of the flow parameters, including areas where the forces are opposite, resulting in fluid stretching and, as a result, negative pressure and strong cavitation with a break of the molecules. This may produce hydrogen from water or be used for water desalination or purification of the sewage waters.

For the US&C facility, it was possible to find simplification of the mathematical model, which allowed obtaining the numerical-analytical solution of the problem for further optimization of the parameters. The future theoretical and experimental research of the described new direction is focused on the regimes with dynamic negative pressure and their influence on the fluid as concerned to cavitation and disintegration of its molecules in a flow.

The considered flows may cause different unique phenomena with applications in energy, chemical technology, etc.

References:
[1] Ivan Kazachkov, Kujtim Hyseni, Mohammad Al Fouzan, Yevgen Chesnokov, Development and application of the device with double rotation turbine, *Proc. 3d Int Conf on Innovative Studies of Contemporary Sciences*. Tokyo, Japan, 2021, February 19-21.

[2] Pascal Belleville, Lhadi Nouri, and Jack Legrand, Mixing Characteristics in the Torus Reactor, *Chem. Eng. Technol*., No.15, 1992, pp. 282–289.

[3] S.T. Wereley & R.M. Lueptow, Inertial particle motion in a Taylor Couette rotating filter, *Phys. Fluids*, 11, 1999, pp. 325.

[4] A. Smits, B. Auvity & M. Sinha, Taylor-Couette flow with a shaped inner cylinder, *Bull. Am. Phys. Soc.*, 45(9), 2000, pp. 37.

[5] A. Andersen, T. Bohr, B. Stenum, J.J. Rasmussen, B. Lautrup Anatomy of bathtub vortex, *Phys. Rev. Lett.*, Vol.91, 2003, pp. 104502-1−4.

[6] CNET. The gaping vortex in this Texas lake is big enough to suck in a boat, [Online]. https://www.cnet.com/science/a-vortex-draining-this-texas-lake-is-like-something-out-of-a-cartoon/ (Accessed Date: Jannuary 11, 2024).

[7] J.S. Hsieh, *Engineering Thermodynamics*. Prentice-Hall, 1993.

[8] Torricelli's experiment. Simple barometer, *PhysicMax*, Retrieved 7 December 2016.

[9] Pascal// *Encyclopedia of Physics*/ Ed. A.M. Prokhorov. M.: Great Russian Encyclopedia, Vol. 3, 1992: Magnetoplasma - Poynting's theorem, pp. 549-550.

[10] Veritasium. The Most Amazing Thing about Trees, [Online]. https://www.tes.com/teaching-resource/the-most-amazing-thing-about-trees-6328295 (Accessed Date: Jannuary 11, 2024).

[11] Simcha Srebnik and Abraham Marmur, Negative Pressure within a Liquid−Fluid Interface Determines Its Thickness, *Langmuir*, vol. 36 (27), 2020, pp. 7943-7947.

[12] R. Attila, Katalin Martinás, L.P.N Rebelo, Thermodynamics of Negative Pressures in Liquids, *J. Non-Equilibrium Thermodynamics*, January, vol. 23, No 4, 1998, pp. 351-375.

[13] W. Kauzmann, *Kinetic theory of gases*, W.A. Benjamin Inc., NY, 1996.

[14] S. Hess, Rheology and shear-induced structures in fluids. In: *Lecture notes in physics 381, Rheological modeling:*

Thermodynamical and statistical approaches. Eds.: Casas-Vasquez J., Jou D., p. 51, Springer-Verlag, Berlin-Heidelberg, 1991.

[15] G.S. Kell, Early observations of negative pressures in liquids. *American J. Phys.*, 51, 1983, pp. 1038.

[16] Q. Zheng, D.J. Durben, G.H. Wolf, C.A. Angel, Liquids at large negative pressures: water at the homogeneous nucleation limit, *Science*, 254, 1991, pp. 829.

[17] D.H. Trevena, *Cavitation and tension in liquids*, Adam Hilger: Bristol, 1987.

[18] H.N.V. Temperley, L.L.G. Chambers, The behavior of water under hydrostatic tension: I, *Proc. Roy. Soc.*, 58, 1946, pp. 420.

[19] H.N.V. Temperley, The behavior of water under hydrostatic tension: II, *Proc. Roy. Soc.*, 58, 1946, pp. 436.

[20] H.N.V. Temperley, The behavior of water under hydrostatic tension: III, *Proc. Roy. Soc.*, 59, 1947, pp. 199.

[21] L.J. Briggs, Limiting negative pressure of water, *J. Appl. Phys.*, 21, 721, 1950.

[22] A.T.J. Hayward, Measuring the extensibility of liquids, *Nature*, 202, 1964, pp. 481.

[23] R.E. Apfel, The tensile strength of liquids, *Sci. Amer.*, 227, 1972, pp. 581.

[24] S.J. Henderson, R.J. Speedy, A Berthelot-Bourdon tube method for studying water under tension, *J. Phys. E. Sci. Instrum.*, 13, 1980, pp. 778.

[25] S.J. Henderson, R.J. Speedy, Temperature of maximum density in water at negative pressure, *J. Phys. Chem.*, 91, 1987, pp. 3062.

[26] S.J. Henderson, R.J. Speedy, Melting temperature of ice at positive and negative pressure, *J. Phys. Chem.*, 91, 1987, pp. 3069.

[27] J.L. Green, D.J. Durben, G.H. Wolf, C.A. Angell, Water and solutions at negative pressure: Raman spectroscopy study to -80 megapascals, *Science*, 249, 1990, pp. 649.

[28] V.E. Vinogradov, E.N. Sinitsin, N.A. Kotelnikov, Effect of Subcooling on the Reaction Force in Discharge of Flashing Water, Fluid Mechanics-Soviet Research, vol. 16, No. 5, 1987, pp. 39-41.

[29] V.E. Vinogradov, S.V. Gissatulina, Ye.N. Sinitsyn, Maximum Tensile Forces in n-Pentane, *Fluid Mechanics Research*, vol. 21, No.4, 1992, pp. 50-54.

[30] V.E. Vinogradov, P.A. Pavlov, Liquid Boiling-up at negative pressures, *Proc. of the Int. Symposium on the Physics of Heat Transfer in Boiling and Condensation,* M., 1997, pp. 57-60.

[31] V.E. Vinogradov, P.A. Pavlov, Limiting superheat of aqueous solutions at negative pressures, *NATO science series*: 2: 42 Math., Physics and Chemistry, Vol. 84: *Liquids under Negative Pressure*, 2002. pp. 13-22.

[32] V.E. Vinogradov, P.A. Pavlov, Cavitation strength of water solutions, *J. of Engineering Thermophysics*, Vol. 11(4), 2002, pp. 353-363.

[33] Ivan V. Kazachkov, Mathematical Modelling and Computer Simulation of the Flow in Thin Gap Channel due to Alternating Volumetric Mass Forces, *WSEAS Transactions on Fluid Mechanics*, Vol. 15, 2020, pp.202-212, https://doi.org/10.37394/232013.2020.15.20.

Contribution of Individual Authors to the Creation of a Scientific Article (Ghostwriting Policy)

Sources of Funding for Research Presented in a Scientific Article or Scientific Article Itself

Conflict of Interest

Creative Commons Attribution License 4.0 (Attribution 4.0 International, CC BY 4.0)